AMERICAN SOCIETY FOR MICROBIOLOGY | Antimicrobial Agents and Chemotherapy®

SUSCEPTIBILITY

# Identification of Antifungal Compounds against Multidrug-Resistant *Candida auris* Utilizing a High-Throughput Drug-Repurposing Screen

**Yu-Shan Cheng,[a] Jose Santinni Roma,[b] Min Shen,[a] Caroline Mota Fernandes,[c] Patricia S. Tsang,[b] He Eun Forbes,[b] Helena Boshoff,[b] Cristina Lazzarini,[c] Maurizio Del Poeta,[c,d,e] Wei Zheng,[a] Peter R. Williamson[b]**

[a]National Center for Advancing Translational Sciences, National Institutes of Health, Bethesda, Maryland, USA
[b]Laboratory of Clinical Immunology and Microbiology, National Institute of Allergy and Infectious Diseases, National Institutes of Health, Bethesda, Maryland, USA
[c]Department of Microbiology and Immunology, Stony Brook University, Stony Brook, New York, USA
[d]Division of Infectious Diseases, Stony Brook University, Stony Brook, New York, USA
[e]Veterans Affairs Medical Center, Northport, New York, USA

**ABSTRACT** *Candida auris* is an emerging fatal fungal infection that has resulted in several outbreaks in hospitals and care facilities. Current treatment options are limited by the development of drug resistance. Identification of new pharmaceuticals to combat these drug-resistant infections will thus be required to overcome this unmet medical need. We have established a bioluminescent ATP-based assay to identify new compounds and potential drug combinations showing effective growth inhibition against multiple strains of multidrug-resistant *Candida auris*. The assay is robust and suitable for assessing large compound collections by high-throughput screening (HTS). Utilizing this assay, we conducted a screen of 4,314 approved drugs and pharmacologically active compounds that yielded 25 compounds, including 6 novel anti-*Candida auris* compounds and 13 sets of potential two-drug combinations. Among the drug combinations, the serine palmitoyltransferase inhibitor myriocin demonstrated a combinational effect with flucytosine against all tested isolates during screening. This combinational effect was confirmed in 13 clinical isolates of *Candida auris*.

**KEYWORDS** *Candida auris*, drug repurposing, drug combination therapy, multidrug resistance

*Candida* species bloodstream infections (candidemia) represent the fourth most common type of bloodstream infection in the United States (1) and have an estimated worldwide prevalence of 25,000 cases annually (2), associated with a 19% to 24% mortality rate (3). *Candida auris* is an emerging, multidrug-resistant fungal species that has recently caused several nosocomial outbreaks in the United States and worldwide (4; see also https://www.cdc.gov/fungal/candida-auris/tracking-c-auris.html). Since its first description in 2009 (5), an increase in cases has been reported globally and is growing relentlessly. In the United States, 988 cases were reported by the end of 2019 according to the Centers for Disease Control and Prevention (CDC), occurring in those who have undergone recent surgery, used invasive medical devices, taken long-term antibiotics, stayed in health care settings, or who have underlying weakened immune systems. The fungus causes invasive infections, especially bloodstream, wound, and ear infections, with high mortality rates ranging from 28% to 56% (6, 7) and is distinguished by its ability to survive for prolonged periods on both patients as well as on inanimate surfaces, making it difficult to eradicate within the hospital environment (8). In addition, while *C. auris* was initially reported in 2009 to be fully

**Citation** Cheng Y-S, Roma JS, Shen M, Mota Fernandes C, Tsang PS, Forbes HE, Boshoff H, Lazzarini C, Del Poeta M, Zheng W, Williamson PR. 2021. Identification of antifungal compounds against multidrug-resistant *Candida auris* utilizing a high-throughput drug-repurposing screen. Antimicrob Agents Chemother 65:e01305-20. https://doi.org/10.1128/AAC.01305-20.



Address correspondence to Wei Zheng, wzheng@mail.nih.gov, or Peter R. Williamson, williamsonpr@mail.nih.gov.

**Received** 30 June 2020
**Returned for modification** 8 September 2020
**Accepted** 31 December 2020
**Accepted manuscript posted online** 19 January 2021
**Published** 18 March 2021

susceptible to clinically relevant antifungals (5), by 2011 resistance to the azole antifungal fluconazole had become evident (9). Currently in the United States, over 90% of cases exhibit elevated MICs to fluconazole (>32 mg/liter), 30% elevated MICs to amphotericin B, and 5% elevated MICs to echinocandins (https://www.cdc.gov/fungal/candida-auris/c-auris-antifungal.html). Most of the isolates are resistant to at least two of the three classes of commonly used antifungal agents (polyenes, azoles, and echinocandins).

Using molecular approaches, *C. auris* has been divided into four distinct geographic clades, namely, South Asian (I), East Asian (II), African (III), South American (IV), and a recently discovered fifth Iranian clade; the East Asian clade predominantly causes ear infection (6, 10). Gene mutations in the *ERG11* gene encoding the target of azole antifungal drugs (cytochrome P450 lanosterol 14$\alpha$-demethylase) are found in the South American (Y132F) and South Asian (Y132F or K143R) clades and are associated with reduced susceptibility to fluconazole (6, 11). In addition, mutations in the ABC transporter *CDR1* and the heat shock protein gene *HSP90* have been linked to azole resistance (12).

Drug repurposing screens have been implemented as an alternative approach to rapidly identify new therapeutics for emerging diseases caused by viruses, bacteria, parasites, and fungi (13–17). Thus, we sought to identify potential new drugs and therapeutic options to combat infections caused by drug-resistant strains of *C. auris*. We report here a new *C. auris* viability assay measuring ATP content in live cells that is robust and capable of high-throughput screening (HTS) of compound libraries. Several new active compounds, as well as sets of potential two drug combinations, were identified after screening 4,314 approved drugs and pharmacologically active compounds using this assay.

## RESULTS

**Optimization of *C. auris* viability assays for HTS.** A high-throughput screening assay was first developed by an adaptation of a standard broth microdilution method for antifungal susceptibility testing of yeasts posted by the Clinical and Laboratory Standards Institute (CLSI) (Fig. 1A) (18). *C. auris* viabilities indicated by both measurement of optical density at 530 nm ($OD_{530}$) and ATP content measurements were determined as endpoint readings that were utilized to quantitate drug responses. The assays were developed using two drug-resistant *C. auris* strains, 0384 and 0390, in a 384-well plate format with two known antifungals, micafungin (20 $\mu$g/ml) and posaconazole (10 $\mu$g/ml), as positive controls. Only the ATP-based assay displayed good signal-to-basal windows between vehicle (dimethyl sulfoxide [DMSO]) and drug-treated groups after a 48-h incubation and thus was selected for the following experiments. Three *C. auris* fungal suspension dilutions at densities of 1:1,000, 1:500, and 1:200 were tested along with two incubation time points of 24 and 48 h (Fig. 1B) in the ATP-based assay. At 24-h, the ATP-based assay signals increased with the increases in fungal densities, while small reductions in signals with increases in fungi densities after 48 h of incubation suggested that a growth plateau was reached under this condition. Micafungin exhibited better growth inhibition than posaconazole at the tested concentrations (Fig. 1C). Under all tested conditions, micafungin treatment reduced the ATP content signals to less than 5% of the DMSO control group for strain 0390. Comparable efficacy (>95% inhibition) for strain 0384 was only achieved when the conditions of low cell density (1 to 1,000 dilution) and short incubation time (24 h) were implemented. Based on the growth curves and the responses to positive-control compounds, 1:1,000 dilution of fungal stocks and a 24-h incubation time were selected for further use in compound screening.

**Screening of the annotated compound library and hit confirmation.** Using the conditions established above, three small-molecule compound libraries, namely the Library of Pharmacologically Active Compounds (LOPAC; 1,279 compounds), NCGC Pharmaceutical Collection (NPC) approved drugs collection (2,816 compounds), and solvent-specific anti-infective drug collection (219 compounds), were screened against

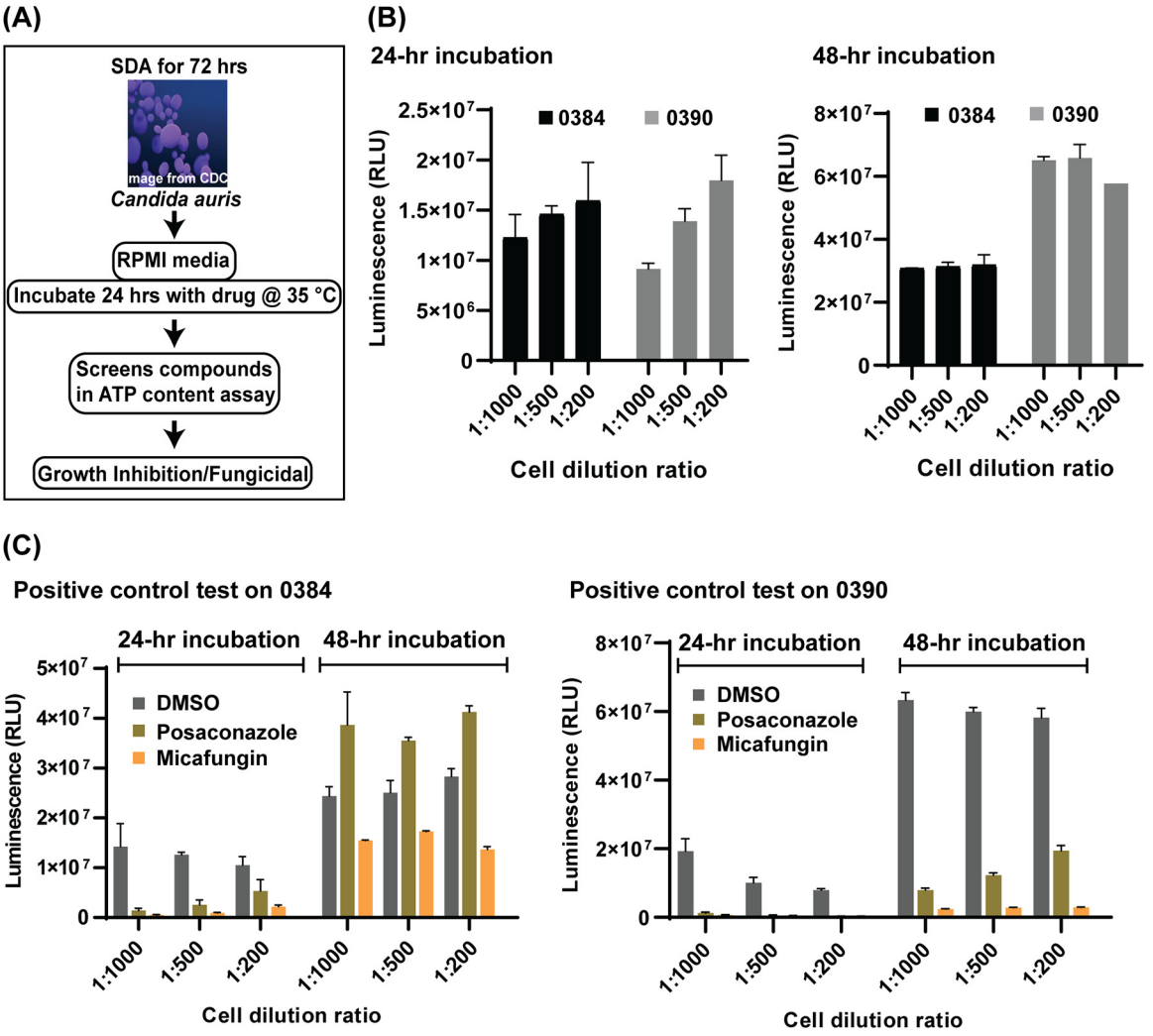


**FIG 1** Workflow and optimization. (A) Scheme of anti-*Candida auris* susceptibility assay. *Candida auris* harvested from colonies grown on Sabouraud dextrose agar (SDA) were incubated in RPMI medium with compounds to identify inhibitors. (B and C) Optimization of the ATP-based antifungal susceptibility assay by fungal density and incubation time. Cells were diluted with fresh medium into ratios of 1 to 1,000, 1 to 500, and 1 to 200 prior to dispensing into assay plates. (B) Fungal growth was detected by an ATP-based assay at 24 and 48 h. (C) Two known compounds, posaconazole and micafungin, were tested against strains 0384 and 0390 to serve as a positive control.

three drug-resistant strains, 0384, 0385, and 0390, in 384-well plates. The parameters of assay quality, including the signal-to-basal ratio, coefficient of variation (CV), and Z′ factor, were monitored using control plates (tested only with the positive control and solvent vehicle). Representative plate data and statistical parameters of each strain are shown in Fig. S1 in the supplemental material. Each compound in the first two libraries was screened at one concentration (7.67 $\mu$M), whereas compounds in the anti-infective compound collection were tested in an 8-point dose titration screen. Compounds showing >40% normalized inhibition against at least one strain were selected for follow-up hit confirmation. A total of 111 compounds were identified in this primary screen, with a hit rate of 2.5%. This set of hits was retested in the same assay in a 11-point concentration-response manner, resulting in 20, 18, and 16 confirmed compounds with >60% normalized inhibition against strains 0384, 0385, and 0390, respectively (half-maximum inhibition concentration [$IC_{50}$] and efficacy values are listed in Table 1). Among these confirmed compounds, 11 were found to be active against all strains (Fig. 2A). These 11 compounds comprise four groups that include

**TABLE 1** Confirmed active compounds against *Candida auris*

| Sample ID[a] | Name | Indication | Activity against *C. auris* strain: 0384 $IC_{50}$ ($\mu$g/ml [$\mu$M]) | 0384 % efficacy | 0385 $IC_{50}$ ($\mu$g/ml [$\mu$M]) | 0385 % efficacy | 0390 $IC_{50}$ ($\mu$g/ml [$\mu$M]) | 0390 % efficacy | Previous report(s) |
|---|---|---|---|---|---|---|---|---|---|
| NCGC00164493-02 | Dipyrithione | Antifungal (topical) | 0.05 (0.22) | 108.64 | 0.06 (0.24) | 99.43 | 0.02 (0.07) | 100.97 | None |
| NCGC00274060-05 | Posaconazole | Antifungal | 0.43 (0.61) | 64.40 | 0.54 (0.77) | 101.94 | 0.96 (1.37) | 94.08 | 22 |
| NCGC00016599-04 | Flucytosine | Antifungal | 0.35 (2.73) | 130.76 | 0.16 (1.22) | 101.77 | 0.13 (0.97) | 108.33 | 21, 22 |
| NCGC00016391-13 | Clioquinol | Antiseptic | 0.59 (1.93) | 125.08 | 0.47 (1.54) | 105.57 | 0.37 (1.22) | 103.97 | 21, 22 |
| NCGC00094815-06 | Broxyquinoline | Antiprotozoal | 0.66 (2.17) | 108.87 | 0.52 (1.72) | 101.32 | 0.47 (1.54) | 101.63 | None |
| NCGC00095264-04 | Chloroxine | Antiseptic | 0.37 (1.72) | 114.05 | 0.33 (1.54) | 106.64 | 0.33 (1.54) | 103.20 | 21, 22 |
| NCGC00018098-09 | Diiodohydroxyquinoline | Antiprotozoal | 1.36 (3.44) | 121.21 | 0.68 (1.72) | 98.07 | 0.61 (1.54) | 93.30 | None |
| NCGC00162165-03 | AC-93253 iodide | Anticancer | 1.39 (3.86) | 108.18 | 1.39 (3.86) | 69.25 | 1.76 (4.86) | 111.62 | None |
| NCGC00017112-10 | Ciclopirox | Antifungal (topical) | 2.12 (7.90) | 132.70 | 2.12 (7.90) | 111.25 | 2.12 (7.90) | 111.82 | 21, 22 |
| NCGC00177980-03 | Oxiconazole nitrate | Antifungal (topical) | 1.90 (3.86) | 80.67 | 2.68 (5.45) | 78.58 | 2.68 (5.45) | 88.12 | None |
| NCGC00178352-06 | Alexidine dihydrochloride | Antiseptic | 3.17 (5.45) | 114.50 | 3.17 (5.45) | 101.61 | 3.17 (5.45) | 117.93 | 21, 22 |
| Against two strains | | | | | | | | | |
| NCGC00091023-11 | Cetylpyridinium (chloride monohydrate) | Antiseptic | 1.66 (5.45) | 98.98 | 1.66 (5.45) | 110.72 | | | None |
| NCGC00163597-04 | Myriocin | Antifungal/ immunomodulator | 0.38 (0.94) | 111.66 | 0.19 (0.47) | 97.38 | | | None |
| NCGC00179034-21 | Pentamidine isethionate | Antiprotozoal | 2.56 (4.33) | 86.61 | 2.88 (4.86) | 111.28 | | | 21 |
| NCGC00179596-03 | Butoconazole nitrate | Antifungal (topical) | 2.31 (4.86) | 69.19 | 2.59 (5.45) | 108.77 | | | None |
| NCGC00025000-09 | Ketoconazole | Antifungal | | | 0.73 (1.37) | 101.06 | 0.92 (1.72) | 96.20 | 21 |
| NCGC00160664-05 | Nitroxoline | Antibiotic | | | 1.04 (5.45) | 101.04 | 1.04 (5.45) | 108.41 | None |
| NCGC00160566-02 | Broquinaldol | Antiprotozoal | | | 1.73 (5.45) | 79.29 | 1.37 (4.33) | 117.37 | None |
| Against one strain | | | | | | | | | |
| NCGC00015360-08 | Pentetic acid | Medical image/internal contamination | 1.05 (2.66) | 107.41 | | | | | 21 |
| NCGC00167430-04 | Tioconazole | Antifungal | 0.75 (1.93) | 73.22 | | | | | 21 |
| NCGC00015251-09 | Clotrimazole | Antifungal (topical) | 1.33 (3.86) | 89.47 | | | | | None |
| NCGC00348215-09 | Bedaquiline (fumarate) | Anti-tuberculosis | 2.40 (4.32) | 62.82 | | | | | None |
| NCGC00159417-06 | Triclosan | Antibacterial/antifungal | 2.95 (10.18) | 61.87 | | | | | None |
| NCGC00164622-04 | Voriconazole | Antifungal | | | | | 1.51 (4.33) | 93.58 | 21, 22 |
| NCGC00169964-05 | Cycloheximide | Antifungal/anticancer | | | | | 0.77 (2.73) | 107.56 | 21 |

[a]ID, identifier.

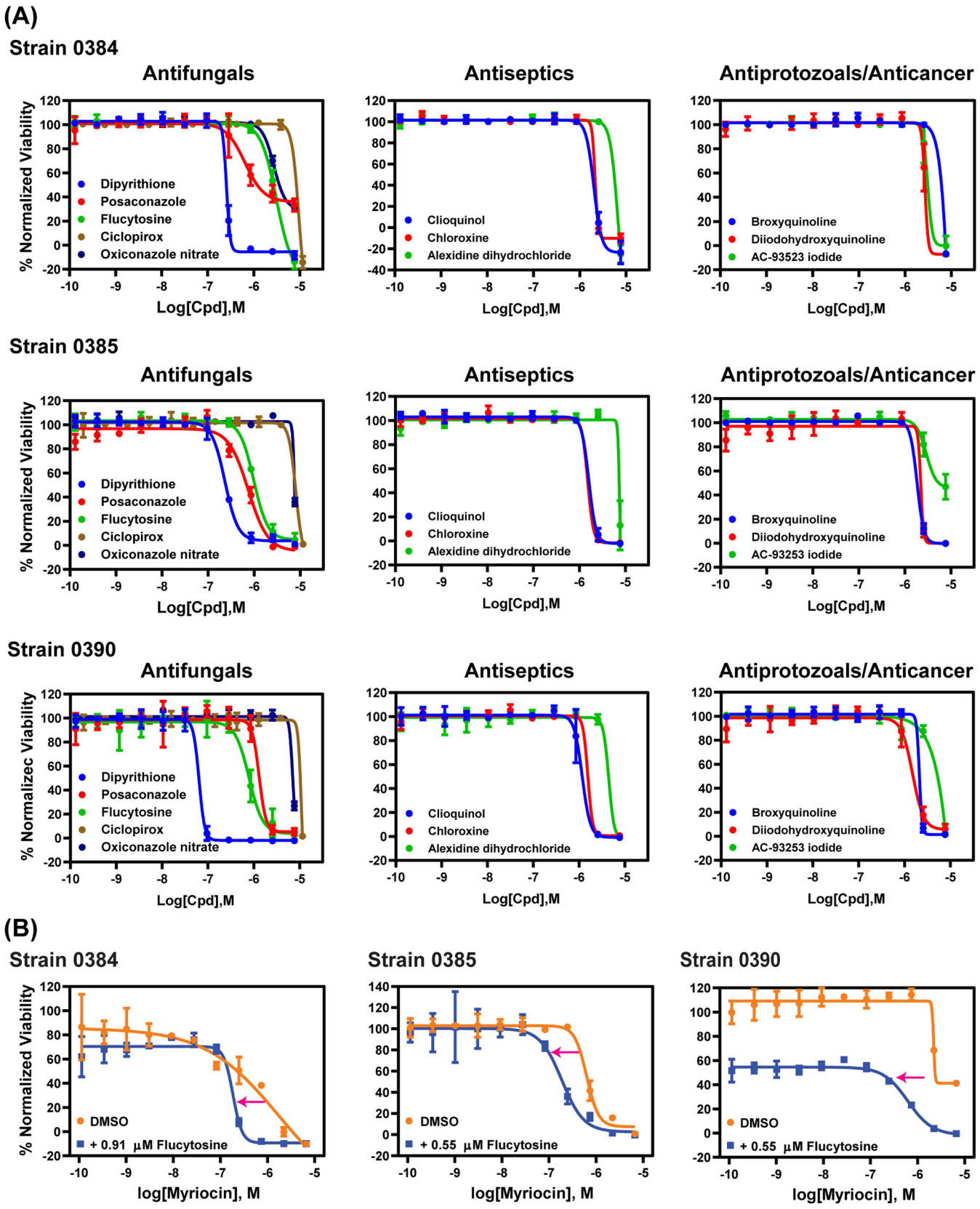


**FIG 2** Concentration-response curves. (A) Concentration-response curves of compounds with pan-activity for all tested strains. Each data point is presented as mean ± standard deviation (SD) for three independent experiments. (B) Concentration-response curves of myriocin with or without flucytosine. Each data point is presented as mean ± standard deviation (SD) for two experiments.

**TABLE 2** Compounds showing at least a 2-fold $IC_{50}$ decrease in the presence of flucytosine

| Compound | $IC_{50}$ ($\mu$M) | | Strain | Flucytosine concn ($\mu$M) |
|---|---|---|---|---|
| | Without flucytosine | With flucytosine | | |
| Myriocin | 1.6 | 0.18 | 0384 | 0.91 |
| Voriconazole | 7.2 | 2.9 | 0384 | 0.91 |
| Posaconazole | 0.45 | 0.15 | 0385 | 0.55 |
| Myriocin | 0.63 | 0.19 | 0385 | 0.55 |
| Broxyquinoline | 0.66 | 0.29 | 0385 | 0.55 |
| Broquinaldol | 2.5 | 0.89 | 0385 | 0.55 |
| Diiodohydroxyquinoline | 1.9 | 0.66 | 0385 | 0.55 |
| Clioquinol | 0.73 | 0.30 | 0385 | 0.55 |
| Broxyquinoline | 0.65 | 0.24 | 0390 | 0.55 |
| Nitroxoline | 6.0 | 2.5 | 0390 | 0.55 |
| Myriocin | 2.2 | 0.62 | 0390 | 0.55 |
| Broquinaldol | 2.1 | 1.1 | 0390 | 0.55 |
| Clioquinol | 0.70 | 0.25 | 0390 | 0.55 |

five antifungals (dipyrithione, posaconazole, flucytosine, ciclopirox, and oxiconazole), three antiseptics (clioquinol, chloroxine, and alexidine dihydrochloride), two antiprotozoals (broxyquinoline and diiodohydroxyquinoline), and one anticancer drug (AC-93253 iodide).

**Drug combination testing.** Because the $IC_{50}$ values of the confirmed hits above were in the micromolar range, drug combinations were then tested to identify compounds that may have synergistic actions against *C. auris*. We excluded dipyrithione from synergistic testing despite its submicromolar potency, since it is a bioactive anti-infective agent limited to topical application in products such as shampoo. Flucytosine is an antifungal agent used for treatment of serious *Candida* infections with an $IC_{50}$ value (0.97 to 2.73 $\mu$M) that is lower than its targeted therapeutic plasma concentrations and which thus may be useful to combine with other drugs identified above. Fourteen compounds were selected to test in combination with flucytosine against strains 0384, 0385, and 0390, including 10 compounds with known antimicrobial activities described above, three clinically useful antifungal agents, and one previously reported to have modest anti-*C. auris* activity (sulfamethoxazole) (19) (see Table S1 in the supplemental material). Concentration response experiments compared the dose-response curves of 14 compounds alone versus those of combinations with 0.55 $\mu$M or 0.91 $\mu$M flucytosine, which represent one-third and one-fifth of the concentrations of the $IC_{50}$ for flucytosine against *C. auris* strain 0384, respectively. These concentrations also exerted more than 50% growth inhibition for strains 0385 and 0390. Among the drug combination sets tested, 13 combinations were found to be additive or synergistic as evidenced by a shift of at least 2-fold in the $IC_{50}$ values toward lower values for these compounds in the presence of flucytosine versus the respective compound alone (Table 2). In the presence of 0.91 $\mu$M flucytosine, the $IC_{50}$ value for voriconazole decreased 2.5-fold from 7.2 $\mu$M to 2.9 $\mu$M for strain 0384. In the presence of 0.55 $\mu$M flucytosine, $IC_{50}$ value of posaconazole decreased 3-fold from 0.45 $\mu$M to 0.15 $\mu$M for strain 0385. The serine palmitoyltransferase inhibitor myriocin increased activity of flucytosine with synergy against all tested strains with flucytosine increasing myriocin activity by 3.3- to 8.9-fold (Fig. 2B). Moreover, most quinoline derivatives yielded increased activity in the range of 2- to 2.9-fold in combination with flucytosine against strains 0385 and 0390.

**Effects of flucytosine and myriocin combination for clinical isolates.** The activities of flucytosine and myriocin combinations on *C. auris* were further assessed in 13 clinical isolates, including those in the screening (Table 3). MICs were determined following the guidelines of the Clinical and Laboratory Standards Institute (CLSI) (18). $MIC_{80}$ values for flucytosine ranged from 0.125 to 0.5 $\mu$g/ml, except against strain 0389 which was highly resistant to flucytosine. $MIC_{80}$ values of myriocin ranged from 0.25 to

**TABLE 3** Antifungal susceptibility profile against flucytosine and myriocin combination

| *C. auris* strain ID | $MIC_{80}$ ($\mu$g/ml) for: Flucytosine | Flucytosine in combination | Myriocin | Myriocin in combination | FICI[a] | Classification |
|---|---|---|---|---|---|---|
| 0381 | 0.5 | 0.25 | 2 | 0.007 | 0.50 | Synergistic |
| 0382 | 0.25 | 0.125 | 2 | 0.007 | 0.50 | Synergistic |
| 0383 | 0.5 | 0.25 | 0.5 | 0.007 | 0.51 | Additive |
| 0384 | 0.5 | 0.25 | 0.5 | 0.007 | 0.51 | Additive |
| 0385 | 0.25 | 0.125 | 0.5 | 0.007 | 0.51 | Additive |
| 0386 | 0.5 | 0.25 | 0.25 | 0.007 | 0.53 | Additive |
| 0387 | 0.125 | 0.06 | 1 | 0.007 | 0.49 | Synergistic |
| 0388 | 0.25 | 0.125 | 2 | 0.007 | 0.50 | Synergistic |
| 0389 | >4 | 4 | 2 | 0.5 | 0.75 | Additive |
| 0390 | 0.25 | 0.125 | 4 | 0.015 | 0.50 | Synergistic |
| 0931 | 0.25 | 0.125 | 0.5 | 0.007 | 0.51 | Additive |
| 1097 | 0.25 | 0.125 | 0.5 | 0.007 | 0.51 | Additive |
| 1099 | 0.5 | 0.25 | 1 | 0.007 | 0.51 | Additive |
| 1100 | 0.25 | 0.125 | 1 | 0.007 | 0.51 | Additive |

[a]FICI, fractional inhibitory concentration index.

4 $\mu$g/ml. In combination treatment, the concentration of flucytosine decreased to 0.06 to 0.25 $\mu$g/ml, except against strain 0389, and the concentration ranges of myriocin were reduced to 0.007 to 0.5 $\mu$g/ml. The fractional inhibitory concentration index (FICI) ranged from 0.49 to 0.53, except against strain 0389, which had an FICI of 0.75, suggesting synergistic and additive effects for all isolates.

**Lipid analysis.** Because of myriocin's known effects on depletion of sphingolipids (20), we sought to study the level of the major sphingolipids (Fig. 3) after inhibition by flucytosine/myriocin combinations by liquid chromatography-mass spectrometry (LC-MS). Three strains, 0384, 0385, and 0390, were analyzed. Among the tested strains, we found significant differences in the levels of dihydrosphingosine (DHS), phytosphingosine (PHS), dihydrosphingosine-1-phosphate (DHS-1-P), phytosphingosine-1-phosphate (PHS-1-P), dihydroceramide (DHC), phytoceramide (PHC), ceramide (CER), and certain species of inositol phosphorylceramide (IPC), whereas no differences were observed for glucosylceramide (GlcCer), which is the most abundant sphingolipid in this yeast (Table 4).

Upon treatment with flucytosine and myriocin, strain 0384 and, to a lesser extent, strains 0385 and 0390, significantly decreased the level of DHS and DHS-1-P (Table 4). Interestingly, upon treatment with flucytosine and myriocin, the level of PHS-1-P increased dramatically in *C. auris* 0385 and 0390, but not in *C. auris* 0384. The levels of dihydroceramide (DHC), phytoceramide (PHC), and ceramide (CER) did not change significantly, except for a decreased level of DHC in *C. auris* 0385 and 0390 (Table 4).

Moreover, the level of all major IPC species (IPC 18:0;3/18:0;0, IPC 18:0;3/24:0;1, and IPC 18:0;3/24:0;2) significantly increased in *C. auris* 0384 when it was treated with flucytosine and myriocin (Table 4). This increase was also observed for IPC 18:0;3/26:0;1 (data not shown). The level of these IPCs did not change in *C. auris* 0385 or 0390 strains upon treatment. The level of glucosylceramide (GlcCer) was not affected by treatment in all tested strains. These results suggest that the levels of sphingolipids among different strains of *C. auris* are much less homogenous than expected. Our results also suggest that treatment with flucytosine and myriocin mostly affects the level of sphingoid bases (DHS, PHS, and their phosphorylated forms), as expected, but also has a significant effect on the level of IPC, although this was only observed in *C. auris* 0384.

## DISCUSSION

In the present study, we applied high-throughput screening of multiple approved drug libraries against three multidrug-resistant *C. auris* strains (0384, 0385, and 0390)

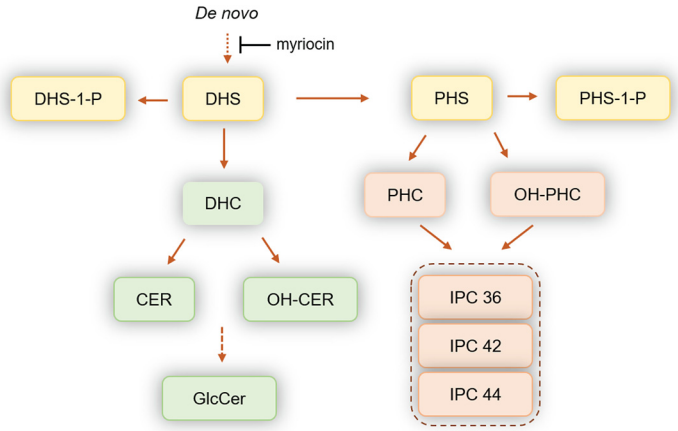


**FIG 3** Schematic representation of the sphingolipid pathways in fungi. All of these reactions are reversible. A dotted line means additional enzymatic steps are present but are not illustrated for clarity. DHS, dihydrosphingosine; PHS, phytosphingosine; DHS-1-P, dihydrosphingosine-1-phosphate; PHS-1-P, phytosphingosine-1-phosphate; DHC, dihydroceramide; PHC, phytoceramide; CER, ceramide; OH-PHC, hydroxylated-phytoceramide; OH-CER, hydroxylated ceramide; GlcCer, glucosylceramide; IPC 36, inositol phosphoryl ceramide containing 36 carbons (sphingoid base plus fatty acid); IPC 42, inositol phosphoryl ceramide containing 42 carbons (sphingoid base plus fatty acid); IPC-44, inositol phosphoryl ceramide containing 44 carbons (sphingoid base plus fatty acid).

to rapidly identity alternative therapeutic candidates. While we were working on this screening in a biosafety level 3 (BSL-3) laboratory, two drug repurposing screens for anti-*C. auris* were reported using a Prestwick approved drug library based on an absorbance assay in a 96-well format (21, 22). Compared to these two reports, we have developed a viability assay measuring ATP content in live *C. auris* in a 384-well plate format that is robust for compound screening, and our approved drug library contains additional approved drugs and drug candidates (4,314 compounds in our collections versus 1,280 compounds in the Prestwick approved drug library). We found a high reproducibility of hits between our results and those reported by Wall et al. (21), validating our methodology when the same strain, 0390, was used. Wall et al. reported 27 hits with >70% inhibition at 20 $\mu$M against *C. auris* strain 0390. Our libraries covered 22 of these 27 hits, and 12 of them demonstrated inhibition in the primary screen (9 validated in confirmation assay) (see Table S2 in the supplemental material).

Eleven compounds demonstrated concentration-dependent growth inhibition for all three tested strains. The five fungicides that comprise the list of active compounds include three topical medicines (dipyrithione, ciclopirox, and oxiconazole nitrate) and two oral drugs (posaconazole and flucytosine). Posaconazole, a triazole antifungal agent, has a MIC breakpoint of 0.06 $\mu$g/ml for *Candida* spp., including *C. albicans*, *C. dubliniensis*, *C. parapsilosis*, and *C. tropicalis*, according to the European Committee on Antimicrobial Susceptibility Testing (23, 24), although a clinical breakpoint for treatment of infections by *C. auris* has not been defined. Fluconazole-resistant fungal strains often exhibit reduced posaconazole susceptibility. Based on experiences in the treatment of invasive aspergillosis, it may not be possible to achieve a therapeutic response when MICs are over 1.0 mg/liter, and a high or elevated dose could be required when the MIC is 0.50 mg/liter (25). The $IC_{50}$ values of posaconazole to drug-resistant *C. auris* ranged from 0.4 to 1 mg/liter in our assay, indicating that posaconazole may be less suitable to treat *C. auris* as a single agent. Flucytosine is a fluorinated pyrimidine analog with potent antifungal activity against *Candida* spp. The 24-h epidemiological cutoff values (ECVs) for flucytosine are 0.5 to 1 mg/liter for some common *Candida* spp., and the susceptible breakpoint of $\leq$1 $\mu$g/ml was established by the British Society for Mycopathology (26). The $IC_{50}$ values for flucytosine ranged from 0.1 to 0.4 mg/liter in

**TABLE 4** Sphingolipid levels in *C. auris* 0384, 0385, and 0390 strains with or without treatment

| | Sphingolipid levels (pmol/pmol Pi) for treatment and strain[a]: | | | | | | | | | | | | | | | | | |
|---|---|---|---|---|---|---|---|---|---|---|---|---|---|---|---|---|---|---|
| | 0384 | | | | | | 0385 | | | | | | 0390 | | | | | |
| | No drug | | 0.06 μg/ml myriocin + 4 μg/ml flucytosine | | 0.25 μg/ml myriocin + 2 μg/ml flucytosine | | No drug | | 0.5 μg/ml myriocin + 2 μg/ml flucytosine | | 1 μg/ml myriocin + 2 μg/ml flucytosine | | No drug | | 1 μg/ml myriocin + 4 μg/ml flucytosine | | 8 μg/ml myriocin + 4 μg/ml flucytosine | |
| Lipid class[b] | Mean | SEM | Mean | SEM | Mean | SEM | Mean | SEM | Mean | SEM | Mean | SEM | Mean | SEM | Mean | SEM | Mean | SEM |
| SPH | 0.00 | 0.00 | 0.00 | 0.00 | 0.00 | 0.00 | 0.00 | 0.00 | 0.00 | 0.00 | 0.00 | 0.00 | 0.48 | 0.09 | 0.54 | 0.10 | 0.51 | 0.10 |
| SPH-1-P | 0.44 | 0.08 | 0.06 | 0.02 | 0.05 | 0.01 | 0.06 | 0.02 | 1.45 | 0.30 | 0.01 | 0.00 | 0.06 | 0.02 | 0.09 | 0.03 | 0.07 | 0.03 |
| DHS | 2.90 | 0.51 | 1.00 | 0.19 | 0.69 | 0.12 | 1.36 | 0.25 | 0.76 | 0.13 | 0.39 | 0.09 | 1.27 | 0.22 | 1.03 | 0.19 | 0.49 | 0.09 |
| DHS-1-P | 1.97 | 0.38 | 0.10 | 0.03 | 0.04 | 0.02 | 0.39 | 0.09 | 0.74 | 0.14 | 0.02 | 0.01 | 0.38 | 0.07 | 0.17 | 0.03 | 0.06 | 0.01 |
| PHS | 0.52 | 0.09 | 0.50 | 0.10 | 0.51 | 0.09 | 0.38 | 0.07 | 0.31 | 0.06 | 0.20 | 0.04 | 1.67 | 0.32 | 2.35 | 0.44 | 2.16 | 0.38 |
| PHS-1-P | 0.36 | 0.06 | 0.15 | 0.03 | 0.06 | 0.02 | 0.02 | 0.01 | 1.18 | 0.24 | 0.00 | 0.00 | 0.81 | 0.15 | 0.53 | 0.18 | 3.72 | 0.79 |
| 18:0;2/18:0;0 DHC | 4.04 | 0.80 | 1.91 | 0.40 | 1.57 | 0.29 | 11.55 | 2.20 | 3.81 | 0.71 | 3.78 | 0.71 | 12.23 | 2.21 | 11.58 | 2.24 | 5.95 | 1.05 |
| 18:1;2/18:0;0 CER | 0.20 | 0.04 | 0.27 | 0.05 | 0.23 | 0.04 | 1.85 | 0.34 | 1.21 | 0.23 | 1.60 | 0.30 | 6.80 | 1.28 | 9.15 | 1.81 | 7.33 | 1.29 |
| 18:2;2/18:0;1 GlcCer | 7.38 | 1.39 | 6.56 | 1.28 | 5.50 | 1.14 | 9.79 | 2.05 | 11.57 | 2.17 | 10.50 | 1.85 | 4.96 | 0.87 | 4.80 | 0.94 | 4.21 | 0.80 |
| 19:2;2/18:0;1 GlcCer | 108.96 | 21.00 | 96.11 | 18.04 | 76.36 | 16.48 | 114.09 | 21.37 | 151.82 | 27.48 | 146.29 | 25.72 | 93.52 | 17.18 | 95.84 | 17.87 | 96.07 | 16.86 |
| 18:0;3/24:1;1 OH-PHC | 14.88 | 2.64 | 16.54 | 3.01 | 15.56 | 2.96 | 15.03 | 2.68 | 12.12 | 2.32 | 16.37 | 3.14 | 11.94 | 2.32 | 17.54 | 3.89 | 10.92 | 2.00 |
| 18:0;3/18:0;0 PHC | 0.15 | 0.03 | 0.16 | 0.03 | 0.16 | 0.03 | 0.97 | 0.18 | 0.84 | 0.17 | 1.00 | 0.21 | 1.31 | 0.27 | 1.94 | 0.38 | 2.01 | 0.36 |
| 18:0;3/24:0;0 PHC | 1.12 | 0.20 | 1.09 | 0.22 | 1.06 | 0.21 | 7.26 | 1.32 | 5.86 | 1.08 | 8.35 | 1.54 | 11.01 | 2.18 | 20.54 | 4.10 | 19.44 | 3.44 |
| 18:0;3/24:0;1 PHC | 1.66 | 0.29 | 1.90 | 0.35 | 1.61 | 0.33 | 4.93 | 0.94 | 3.97 | 0.76 | 6.01 | 1.05 | 2.39 | 0.43 | 2.72 | 0.57 | 3.10 | 0.54 |
| IPC 36C - 18:0;2/18:0;0 | 0.70 | 0.13 | 0.51 | 0.09 | 0.83 | 0.18 | 0.87 | 0.16 | 0.50 | 0.09 | 0.30 | 0.06 | 2.39 | 0.43 | 0.91 | 0.16 | 0.83 | 0.16 |
| IPC 36C - 18:0;3/18:0;0 | 1.23 | 0.22 | 1.68 | 0.30 | 3.44 | 0.71 | 0.34 | 0.06 | 0.36 | 0.06 | 0.27 | 0.05 | 0.68 | 0.14 | 0.49 | 0.09 | 0.37 | 0.06 |
| IPC 36C - 18:0;3/18:0;1 | 0.30 | 0.06 | 0.41 | 0.07 | 0.72 | 0.16 | 0.17 | 0.03 | 0.20 | 0.04 | 0.15 | 0.03 | 0.11 | 0.02 | 0.10 | 0.02 | 0.13 | 0.02 |
| IPC 42C - 18:0;3/24:0;1 | 5.76 | 1.10 | 5.11 | 1.09 | 17.26 | 3.62 | 2.73 | 0.49 | 2.62 | 0.46 | 2.69 | 0.50 | 2.41 | 0.43 | 2.72 | 0.49 | 2.69 | 0.58 |
| IPC 44C - 18:0;3/24:0;2 | 5.11 | 0.99 | 4.51 | 0.97 | 16.35 | 3.39 | 4.20 | 0.76 | 4.45 | 0.78 | 4.69 | 0.94 | 2.96 | 0.53 | 2.81 | 0.53 | 2.50 | 0.48 |
| IPC 44C - 18:0;3/26:0;1 | 3.65 | 0.68 | 2.73 | 0.58 | 14.54 | 3.21 | 4.10 | 0.89 | 2.78 | 0.49 | 3.47 | 0.62 | 4.32 | 0.89 | 3.91 | 0.76 | 3.65 | 0.64 |
| IPC 44C - 18:0;3/26:0;2 | 1.30 | 0.25 | 1.01 | 0.20 | 5.07 | 1.10 | 1.17 | 0.21 | 1.03 | 0.19 | 1.33 | 0.25 | 1.04 | 0.19 | 1.19 | 0.22 | 0.63 | 0.12 |

[a]Pi, inorganic phosphate.

[b]SPH, sphingosine; SPH-1-P, sphingosine-1-phosphate; DHS, dihydrosphingosine; DHS-1-P, dihydrosphingosine-1-phosphate; PHS, phytosphingosine; PHS-1-P, phytosphingosine-1-phosphate; DHC, dihydroceramide; CER, ceramide; GlcCer, glucosylceramide; OH-PHC, hydroxylated-phytoceramide; PHC, phytoceramide; IPC, inositol phosphoryl ceramide.

our assay, but the MIC value listed in the CDC panel against strain 0390 is >128 mg/liter. The discrepancy could be due to the different assay period (24 h versus 48 h) used in the experiments. Nevertheless, according to our results, flucytosine in combination could be a potential treatment option for drug-resistant *C. auris*. However, significant toxicity would likely reserve its use for the most resistant infections.

In addition to antifungal agents, our screens identified six novel compounds with anti-*C. auris* activity. More significantly, four of them are quinoline derivatives, specifically 8-hydroxyquinolines, indicating their potential application to treat infections by *C. auris*. It is noteworthy that diiodohydroxyquinoline was also observed in the report by Wall et al. (21). 8-Hydroxyquinolines have diverse therapeutic applications, including neuroprotection, anticancer, anti-inflammatory, and antimicrobial effects. Their antimicrobial activities have been reported to encompass broad-spectrum antibacterial, antimalarial, and antiviral activities (27). The fungicidal activity of 8-hydroxyquinolines has also been recognized recently (28–30), although the mechanism of action of hydroxyquinolines against *Candida* spp. has not been fully characterized. Pippi et al. showed that clioquinol can damage fungal cell walls and inhibit the formation of pseudohyphae in *C. albicans* (31). However, these results need to be further validated, as *C. auris* and *C. albicans* do not share the same propensity to induce filament formation (32, 33). Another study, published by Yaakov et al., investigated the mechanisms of broxyquinoline in *Aspergillus fumigatus*; they concluded that broxyquinoline bound to iron, copper, or zinc which coordinated into the active site of metalloenzymes, particularly oxidoreductases, causing enzyme malfunction that resulted in oxidative stress and apoptosis in *A. fumigatus* (34).

Even though flucytosine appears to be a potent compound against multidrug-resistant *C. auris*, clinical application as flucytosine monotherapy is limited due to the rapid development of drug resistance (35). A previous study of drug combination therapy using a checkerboard assay demonstrated that flucytosine exhibited an indifferent interaction with different classes of antifungals, including a polyene (amphotericin B), an echinocandin (micafungin), and an azole (voriconazole), against 14 *C. auris* isolates (36). In line with this report, two azole compounds (voriconazole and posaconazole) in a combination with flucytosine yielded indifferent interactions against *C. auris* strains 0384 and 0385 based on the values of FICI at $IC_{50}$.

Intriguingly, we found that flucytosine leads to an increase in the activity of myriocin against all three *C. auris* strains. In the profiling study, a combination of flucytosine and myriocin showed synergistic effects in five strains and additive effects in eight strains. Myriocin is a metabolite derived from thermophilic fungi. It is a sphingosine analog and a potent inhibitor of serine palmitoyltransferase and thus blocks sphingolipid biosynthesis (Fig. 3). Fingolimod, a derivative of myriocin, was approved by the Food and Drug Administration (FDA) as an immunomodulating drug to treat multiple sclerosis. Myriocin's antifungal activity against *C. albicans* was found when it was discovered in 1973 (37). However, the same report revealed a toxicity in mice that is due to a shared molecular target between mammals and fungi, the enzyme serine palmitoyltransferase.

Additional studies sought to determine the cellular levels of sphingolipids after flucytosine and myriocin treatment to characterize the targeted molecular pathways in this peculiarly resistant fungus. These studies revealed a decrease in sphingoid bases, as expected, but, interestingly, the combination treatment significantly increased the level of IPC species in *C. auris* 0384. This could have occurred either by an upregulation of inositol phosphorylceramide (IPC) synthase activity, which is unlikely because the level of ceramides (substrates of the IPC synthase) does not decrease, or by a downregulation of Isc1 activity, the enzyme performing the reverse reaction of hydrolyzing IPCs into ceramide (38, 39). It is interesting that this was not observed in *C. auris* strains 0385 and 0390, suggesting the specificity of this effect in strain 0384. Another interesting observation was an increase in PHS-1-P in strains 0385 and 0390, which was likely due to a toxic effect of the drugs on the cells, particularly the lytic drug flucytosine,

primarily because specific enzyme inhibition would presumably result in elevation of DHS-1-P levels, since the known metabolic enzymes metabolize both species. The sphingolipid analysis also revealed differences within different classes of pathogenic fungi. For example, two species of GlcCer were detectable in *C. auris* in addition to an unmethylated form, the latter of which is typically undetectable in *Cryptococcus* spp., *Candida albicans*, or *Aspergillus* spp. (39, 40). In addition, GlcCer appeared to be the most abundant sphingolipid in *C. auris*, more similarly to *Cryptococcus* than to other *Candida* species such as *C. albicans* that make more complex species of IPCs containing more sugars (e.g., 1-3 mannose and 1-3 inositol) attached to the ceramide backbone (41). Clearly, further studies are needed to understand the unique enzymatic kinetics of sphingolipid pathways in *C. auris* versus those of other fungi and upon sphingosine-related treatment regimens that may potentiate antifungal drug development of this novel pathway, as recently demonstrated in *Cryptococcus neoformans* (42).

In summary, we reported a viability assay measuring ATP content in live *C. auris* for high-throughput screening of approved drug collections. This assay is robust and easy to perform in any academic HTS laboratory and could be useful to screen large compound libraries for lead discovery, as well as individual patient isolates to identify personalized treatment options for a given patient with an intractable, resistant infection, as recently performed for a patient whose carbapenem-resistant *Escherichia coli* bacterial infection and a specific drug toxicity restricted therapeutic options (43, 44). In the present study, we have identified 6 compounds with novel anti-*C. auris* activities. We also found 13 sets of drug combinations that enhanced activity of individual drugs against *C. auris*, including the pairs flucytosine-myriocin, flucytosine-broxyquinoline, flucytosine-broquinaldol, and flucytosine-clioquinol. The additive/synergistic effect of the flucytosine-myriocin combination was demonstrated in 13 clinical isolates. These drug combination pairs may have potential to be used clinically to treat refractory infections caused by drug-resistant *C. auris*.

## MATERIALS AND METHODS

**Materials.** Micafungin sodium (catalog no. GN26615) was purchased from Aurum Pharmatech LLC (Franklin Park, NJ). Posaconazole (catalog no. 32103) was obtained from Sigma-Aldrich (St. Louis, MO). The ATP-based kit (BacTiter-Glo microbial cell viability assay, catalog no. G8231) was purchased from Promega (Madison, WI). The 384-well white sterile plates (catalog no. 781073) were purchased from Greiner Bio-One (Monroe, NC). RPMI 1640 medium was customized by K-D Medical (Columbia, MD).

**Preparation of fungal stocks.** *C. auris* strains were obtained from the CDC. Recovery procedures were taken from instructions provided by CDC and the FDA AR Isolate Bank. Frozen stocks were subcultured onto Sabouraud dextrose agar plates for 72 h at 30°C. For each strain, three colonies were inoculated into 10 ml fresh RPMI 1640 medium for 48 h at 30°C. Once cultures reached an absorbance (530 nm) of 0.3 to 0.5, sterile glycerol was added to a final concentration of 10%. The 10% glycerol stocks were aliquoted and stored at −80°C.

**ATP-based antifungal screening assays.** The BacTiter-Glo microbial cell viability assay kit, consisting of luciferase/luciferin and detergents, was used to quantify the amount of ATP representing the cell viability (see Table S3 in the supplemental material). For assay development, frozen *C. auris* stocks were thawed at 4°C and diluted with RPMI 1640 medium in ratios of 1:1,000, 1:500, and 1:200 prior to plating into wells. *C. auris* cells were incubated for 24 h and 48 h at 35°C in a 5% $CO_2$ humidified atmosphere.

**Compound library and liquid handling instrument.** The library of 1,280 pharmacologically active compounds (LOPAC, Sigma) contains a collection of 1,280 small molecules with characterized biological activities that has been widely used for HTS assay validations (45, 46). The NIH Chemical Genomics Center Pharmaceutical (NPC) collection was constructed in-house and comprises 2,816 compounds that have been approved for use by the Food and Drug Administration, along with a number of approved molecules from related agencies in foreign countries (47). A solvent-specific anti-infective compound collection was built in-house with 219 compounds, including antibiotic, antiviral, antifungal, antiparasitic, and other reported anti-infective drugs. Based on their solubility, compounds were prepared as an eight-point 1:3 serial dilution in water (45 compounds) or DMSO (174 compounds) and stored separately.

**Susceptibility testing.** MICs were determined following the guidelines of the Clinical and Laboratory Standards Institute (CLSI) (18). *C. auris* strains were grown in RPMI medium, buffered with morpholinepropanesulfonic acid (MOPS) to pH 7.0. Flucytosine and myriocin were serially diluted from 32 to 0.03 $\mu$g/ml, while fluconazole and caspofungin were serially diluted from 64 to 0.06 $\mu$g/ml in a 96-well plate. The inoculum was prepared according to CLSI methods (48). After 48 h of incubation at 35°C, the absorbance at 450 nm was read. The $MIC_{80}$ was established as the lowest concentration of each compound inhibiting 80% of fungal growth.

The effects of the flucytosine and myriocin combination were assessed by a checkerboard microdilution method and classified by the FICI (49). In a 96-well plate, myriocin was serially diluted from 8 $\mu$g/ml to 0.007 $\mu$g/ml (11 dilutions), while flucytosine was serially diluted from 4 $\mu$g/ml to 0.06 $\mu$g/ml (7 dilutions). The FICI was calculated as follows: (MIC of myriocin in combination/MIC of myriocin alone) + (MIC of flucytosine in combination/MIC of flucytosine alone). For calculation purposes, the MIC of flucytosine for *C. auris* 0389 strain was defined as 8 $\mu$g/ml. The interaction was considered synergistic when the FICI was $\leq$0.5, additive when the FICI was $>$0.5 and $\leq$4, and antagonistic when the FICI was $>$4 (49).

**Lipid analysis.** The yeast colonies were inoculated in 50 ml yeast nitrogen base (YNB) medium plus 5% asparagine and placed on a rotary shaker at 30°C for 16 h. The cultures were then washed 3 times in phosphate-buffered saline (PBS), resuspended, and counted. A final concentration of $5 \times 10^8$ cells was resuspended in 1 ml of YNB medium containing different concentrations of myriocin and flucytosine, namely, 0.06/4 $\mu$g/ml and 0.25/2 $\mu$g/ml, for strain 384; 0.5/2 $\mu$g/ml and 1/2 $\mu$g/ml for strain 385; and 1/4 $\mu$g/ml and 8/4 $\mu$g/ml for strain 390. A control containing only YNB with yeast cells (no drug) was added. All the samples were processed in triplicate. The samples were incubated on a rotary shaker at 37°C and 5% $CO_2$ for 3 h. After 3 h, the cultures were pelleted down to remove the medium and processed for lipid extraction. The lipid extraction protocol consisted of 3 steps, as follows: (i) Mandala extraction, (ii) Bligh and Dyer protocol, and (iii) base hydrolysis. At the end of the Bligh and Dyer step, an aliquot was taken for the determination of the inorganic phosphate (Pi) content, which was used to normalized the data obtained from the liquid chromatography-mass spectrometry (LC-MS). After base hydrolysis, the samples were dried and sent to the LC-MS facility for analysis. Appropriate lipid standards were used for quantitative analysis. Statistical analysis was performed by two-way analysis of variance (ANOVA). A $P$ value of $<$0.05 was considered to be significant.

**Data analysis.** Data from the primary screen and the confirmation screen were analyzed using a software developed in-house at the NIH Chemical Genomics Center (NCGC) (50). Briefly, raw plate reads were normalized relative to the DMSO-only wells (100% viability) and 20 $\mu$g/ml micafungin-treated wells (0% viability). Each data set was corrected using the DMSO plate by applying an in-house pattern correction algorithm. The half-maximum inhibition concentration ($IC_{50}$) values and % efficacy were obtained by fitting the concentration-response titration data to a 4-parameter Hill equation (51).

Dose-response curves were generated using Prism 8 (GraphPad Software, Inc., San Diego, CA). Results in the figures were expressed as mean $\pm$ standard deviation (SD).

## SUPPLEMENTAL MATERIAL

Supplemental material is available online only.

**SUPPLEMENTAL FILE 1**, PDF file, 0.4 MB.

## ACKNOWLEDGMENTS

We thank Hui Guo for assistance with the data processing.

This work was supported by the Intramural Research Program of National Center for Advancing Translational Sciences, National Institutes of Health (NIH) (W.Z.), and National Institutes of Allergy and Infectious Diseases, National Institutes of Health (NIH) (P.R.W.). This work was also supported, in part, by NIH grants AI136934 and AI125770 and by Merit Review Grant I01BX002924 from the Veterans Affairs Program to M.D.P.

M.D.P. is a cofounder and chief scientific officer (CSO) of MicroRid Technologies, Inc.

## REFERENCES

1. Magill SS, O'Leary E, Janelle SJ, Thompson DL, Dumyati G, Nadle J, Wilson LE, Kainer MA, Lynfield R, Greissman S, Ray SM, Beldavs Z, Gross C, Bamberg W, Sievers M, Concannon C, Buhr N, Warnke L, Maloney M, Ocampo V, Brooks J, Oyewumi T, Sharmin S, Richards K, Rainbow J, Samper M, Hancock EB, Leaptrot D, Scalise E, Badrun F, Phelps R, Edwards JR. 2018. Changes in prevalence of health care-associated infections in U.S. hospitals. N Engl J Med 379:1732–1744. https://doi.org/10.1056/NEJMoa1801550.
2. Tsay S, Williams S, Mu Y, Epson E, Johnston H, Farley MM, Harrison LH, Vonbank B, Shrum S, Dumyati G, Zhang A, Schaffner W, Magill S, Vallabhaneni S. 2018. National burden of candidemia, United States, 2017. Open Forum Infect Dis 5:S142–3. https://doi.org/10.1093/ofid/ofy210.374.
3. Morgan J, Meltzer MI, Plikaytis BD, Sofair AN, Huie-White S, Wilcox S, Harrison LH, Seaberg EC, Hajjeh RA, Teutsch SM. 2005. Excess mortality, hospital stay, and cost due to candidemia: a case-control study using data from population-based candidemia surveillance. Infect Control Hosp Epidemiol 26:540–547. https://doi.org/10.1086/502581.
4. Wickes BL. 2020. Analysis of a *Candida auris* outbreak provides new insights into an emerging pathogen. J Clin Microbiol 58:e02083-19. https://doi.org/10.1128/JCM.02083-19.
5. Satoh K, Makimura K, Hasumi Y, Nishiyama Y, Uchida K, Yamaguchi H. 2009. *Candida auris* sp. nov., a novel ascomycetous yeast isolated from the external ear canal of an inpatient in a Japanese hospital. Microbiol Immunol 53:41–44. https://doi.org/10.1111/j.1348-0421.2008.00083.x.
6. Lockhart SR, Etienne KA, Vallabhaneni S, Farooqi J, Chowdhary A, Govender NP, Colombo AL, Calvo B, Cuomo CA, Desjardins CA, Berkow EL, Castanheira M, Magobo RE, Jabeen K, Asghar RJ, Meis JF, Jackson B, Chiller T, Litvintseva AP. 2017. Simultaneous emergence of multidrug-resistant *Candida auris* on 3 continents confirmed by whole-genome sequencing and epidemiological analyses. Clin Infect Dis 64:134–140. https://doi.org/10.1093/cid/ciw691.
7. Calvo B, Melo AS, Perozo-Mena A, Hernandez M, Francisco EC, Hagen F, Meis JF, Colombo AL. 2016. First report of *Candida auris* in America: clinical and microbiological aspects of 18 episodes of candidemia. J Infect 73:369–374. https://doi.org/10.1016/j.jinf.2016.07.008.
8. Eyre DW, Sheppard AE, Madder H, Moir I, Moroney R, Quan TP, Griffiths D, George S, Butcher L, Morgan M, Newnham R, Sunderland M, Clarke T, Foster D, Hoffman P, Borman AM, Johnson EM, Moore G, Brown CS, Walker AS, Peto TEA, Crook DW, Jeffery KJM. 2018. A *Candida auris* outbreak and its control in an intensive care setting. N Engl J Med 379:1322–1331. https://doi.org/10.1056/NEJMoa1714373.
9. Lee WG, Shin JH, Uh Y, Kang MG, Kim SH, Park KH, Jang HC. 2011. First three reported cases of nosocomial fungemia caused by *Candida auris*. J Clin Microbiol 49:3139–3142. https://doi.org/10.1128/JCM.00319-11.

10. Chow NA, de Groot T, Badali H, Abastabar M, Chiller TM, Meis JF. 2019. Potential fifth clade of *Candida auris*, Iran, 2018. Emerg Infect Dis 25:1780–1781. https://doi.org/10.3201/eid2509.190686.
11. Healey KR, Kordalewska M, Jimenez Ortigosa C, Singh A, Berrio I, Chowdhary A, Perlin DS. 2018. Limited ERG11 mutations identified in isolates of *Candida auris* directly contribute to reduced azole susceptibility. Antimicrob Agents Chemother 62:e01427-18. https://doi.org/10.1128/AAC.01427-18.
12. Kim SH, Iyer KR, Pardeshi L, Munoz JF, Robbins N, Cuomo CA, Wong KH, Cowen LE. 2019. Genetic analysis of *Candida auris* implicates Hsp90 in morphogenesis and azole tolerance and Cdr1 in azole resistance. mBio 10:e02529-18. https://doi.org/10.1128/mBio.00346-19.
13. Rabjohns JLA, Park YD, Dehdashti J, Henderson C, Zelazny A, Metallo SJ, Zheng W, Williamson PR. 2014. A high-throughput screening assay for fungicidal compounds against *Cryptococcus neoformans*. J Biomol Screen 19:270–277. https://doi.org/10.1177/1087057113496847.
14. Sun W, Park YD, Sugui JA, Fothergill A, Southall N, Shinn P, McKew JC, Kwon-Chung KJ, Zheng W, Williamson PR. 2013. Rapid identification of antifungal compounds against *Exserohilum rostratum* using high throughput drug repurposing screens. PLoS One 8:e70506. https://doi.org/10.1371/journal.pone.0070506.
15. Sun W, Huang X, Li H, Tawa G, Fisher E, Tanaka TQ, Shinn P, Huang W, Williamson KC, Zheng W. 2017. Novel lead structures with both *Plasmodium falciparum* gametocytocidal and asexual blood stage activity identified from high throughput compound screening. Malar J 16:147. https://doi.org/10.1186/s12936-017-1805-0.
16. Sun W, Weingarten RA, Xu M, Southall N, Dai S, Shinn P, Sanderson PE, Williamson PR, Frank KM, Zheng W. 2016. Rapid antimicrobial susceptibility test for identification of new therapeutics and drug combinations against multidrug-resistant bacteria. Emerg Microbes Infect 5:e116. https://doi.org/10.1038/emi.2016.123.
17. Sun W, He S, Martinez-Romero C, Kouznetsova J, Tawa G, Xu M, Shinn P, Fisher E, Long Y, Motabar O, Yang S, Sanderson PE, Williamson PR, Garcia-Sastre A, Qiu X, Zheng W. 2017. Synergistic drug combination effectively blocks Ebola virus infection. Antiviral Res 137:165–172. https://doi.org/10.1016/j.antiviral.2016.11.017.
18. Clinical and Laboratory Standards Institute. 2008. Reference method for broth dilution antifungal susceptibility testing of yeasts; approved standard, 3rd ed. CLSI document M27-A3. Clinical and Laboratory Standards Institute, Wayne, PA.
19. Eldesouky HE, Li X, Abutaleb NS, Mohammad H, Seleem MN. 2018. Synergistic interactions of sulfamethoxazole and azole antifungal drugs against emerging multidrug-resistant *Candida auris*. Int J Antimicrob Agents 52:754–761. https://doi.org/10.1016/j.ijantimicag.2018.08.016.
20. Mota Fernandes C, Del Poeta M. 2020. Fungal sphingolipids: role in the regulation of virulence and potential as targets for future antifungal therapies. Expert Rev Anti Infect Ther 18:1083–1092. https://doi.org/10.1080/14787210.2020.1792288.
21. Wall G, Chaturvedi AK, Wormley FL, Wiederhold NP, Patterson HP, Patterson TF, Lopez-Ribot JL. 2018. Screening a repurposing library for inhibitors of multidrug-resistant *Candida auris* Identifies ebselen as a repositionable candidate for antifungal drug development. Antimicrob Agents Chemother 62:e01084-18. https://doi.org/10.1128/AAC.01084-18.
22. de Oliveira HC, Monteiro MC, Rossi SA, Peman J, Ruiz-Gaitan A, Mendes-Giannini MJS, Mellado E, Zaragoza O. 2019. Identification of off-patent compounds that present antifungal activity against the emerging fungal pathogen *Candida auris*. Front Cell Infect Microbiol 9:83. https://doi.org/10.3389/fcimb.2019.00083.
23. Arendrup MC, Cuenca-Estrella M, Donnelly JP, Hope W, Lass-Florl C, Rodriguez-Tudela JL, European Committee on Antimicrobial Susceptibility Testing–Subcommittee on Antifungal Susceptibility Testing (EUCAST-AFST). 2011. EUCAST technical note on posaconazole. Clin Microbiol Infect 17:E16–E17. https://doi.org/10.1111/j.1469-0691.2011.03646.x.
24. European Committee on Antimicrobial Susceptibility Testing. 2020. Breakpoint tables for interpretation of MICs for antifungal agents, version 10.0.
25. Dekkers BGJ, Bakker M, van der Elst KCM, Sturkenboom MGG, Veringa A, Span LFR, Alffenaar JWC. 2016. Therapeutic drug monitoring of posaconazole: an update. Curr Fungal Infect Rep 10:51–61. https://doi.org/10.1007/s12281-016-0255-4.
26. Pfaller MA, Espinel-Ingroff A, Canton E, Castanheira M, Cuenca-Estrella M, Diekema DJ, Fothergill A, Fuller J, Ghannoum M, Jones RN, Lockhart SR, Martin-Mazuelos E, Melhem MSC, Ostrosky-Zeichner L, Pappas P, Pelaez T, Peman J, Rex J, Szeszs MW. 2012. Wild-type MIC distributions and epidemiological cutoff values for amphotericin B, flucytosine, and itraconazole and *Candida* spp. as determined by CLSI broth microdilution. J Clin Microbiol 50:2040–2046. https://doi.org/10.1128/JCM.00248-12.
27. Prachayasittikul V, Prachayasittikul S, Ruchirawat S, Prachayasittikul V. 2013. 8-Hydroxyquinolines: a review of their metal chelating properties and medicinal applications. Drug Des Devel Ther 7:1157–1178. https://doi.org/10.2147/DDDT.S49763.
28. Gershon H, Gershon M, Clarke DD. 2002. Antifungal activity of substituted 8-quinolinol-5- and 7-sulfonic acids: a mechanism of action is suggested based on intramolecular synergism. Mycopathologia 155:213–217. https://doi.org/10.1023/a:1021166500169.
29. Pippi B, Reginatto P, Machado G, Bergamo VZ, Lana DFD, Teixeira ML, Franco LL, Alves RJ, Andrade SF, Fuentefria AM. 2017. Evaluation of 8-hydroxyquinoline derivatives as hits for antifungal drug design. Med Mycol 55:763–773. https://doi.org/10.1093/mmy/myx003.
30. Pippi B, Merkel S, Staudt KJ, Teixeira ML, de Araujo BV, Zanette RA, Andrade SF, Fuentefria AM. 2019. Oral clioquinol is effective in the treatment of a fly model of *Candida* systemic infection. Mycoses 62:475–481. https://doi.org/10.1111/myc.12888.
31. Pippi B, Lopes W, Reginatto P, Silva FÉK, Joaquim AR, Alves RJ, Silveira GP, Vainstein MH, Andrade SF, Fuentefria AM. 2019. New insights into the mechanism of antifungal action of 8-hydroxyquinolines. Saudi Pharm J 27:41–48. https://doi.org/10.1016/j.jsps.2018.07.017.
32. Bravo Ruiz G, Ross ZK, Gow NAR, Lorenz A. 2020. Pseudohyphal growth of the emerging pathogen *Candida auris* is triggered by genotoxic stress through the S phase checkpoint. mSphere 5:e00151-20. https://doi.org/10.1128/mSphere.00151-20.
33. Wang X, Bing J, Zheng Q, Zhang F, Liu J, Yue H, Tao L, Du H, Wang Y, Wang H, Huang G. 2018. The first isolate of *Candida auris* in China: clinical and biological aspects. Emerg Microbes Infect 7:93. https://doi.org/10.1038/s41426-018-0095-0.
34. Ben Yaakov D, Shadkchan Y, Albert N, Kontoyiannis DP, Osherov N. 2017. The quinoline bromoquinol exhibits broad-spectrum antifungal activity and induces oxidative stress and apoptosis in *Aspergillus fumigatus*. J Antimicrob Chemother 72:2263–2272. https://doi.org/10.1093/jac/dkx117.
35. Vermes A, Guchelaar HJ, Dankert J. 2000. Flucytosine: a review of its pharmacology, clinical indications, pharmacokinetics, toxicity and drug interactions. J Antimicrob Chemother 46:171–179. https://doi.org/10.1093/jac/46.2.171.
36. Bidaud AL, Botterel F, Chowdhary A, Dannaoui E. 2019. *In vitro* antifungal combination of flucytosine with amphotericin B, voriconazole, or micafungin against *Candida auris* shows no antagonism. Antimicrob Agents Chemother 63:e01393-19. https://doi.org/10.1128/AAC.01393-19.
37. Kluepfel D, Bagli J, Baker H, Charest MP, Kudelski A. 1972. Myriocin, a new antifungal antibiotic from *Myriococcum albomyces*. J Antibiot (Tokyo) 25:109–115. https://doi.org/10.7164/antibiotics.25.109.
38. Henry J, Guillotte A, Luberto C, Del P. 2011. Characterization of inositol phospho-sphingolipid-phospholipase C 1 (Isc1) in *Cryptococcus neoformans* reveals unique biochemical features. FEBS Lett 585:635–640. https://doi.org/10.1016/j.febslet.2011.01.015.
39. Matmati N, Hannun YA. 2008. Thematic review series: sphingolipids. ISC1 (inositol phosphosphingolipid-phospholipase C), the yeast homologue of neutral sphingomyelinases. J Lipid Res 49:922–928. https://doi.org/10.1194/jlr.R800004-JLR200.
40. Mota Fernandes C, Goldman GH, Del Poeta M. 2018. Biological roles played by sphingolipids in dimorphic and filamentous fungi. mBio 9:e00642-18. https://doi.org/10.1128/mBio.00642-18.
41. Singh A, Del Poeta M. 2016. Sphingolipidomics: an important mechanistic tool for studying fungal pathogens. Front Microbiol 7:501. https://doi.org/10.3389/fmicb.2016.00501.
42. Bryan AM, You JK, McQuiston T, Lazzarini C, Qiu Z, Sheridan B, Nuesslein-Hildesheim B, Del Poeta M. 2020. FTY720 reactivates cryptococcal granulomas in mice through S1P receptor 3 on macrophages. J Clinical Invest 130:4546–4560. https://doi.org/10.1172/JCI136068.
43. Cheng YS, Williamson PR, Zheng W. 2019. Improving therapy of severe infections through drug repurposing of synergistic combinations. Curr Opin Pharmacol 48:92–98. https://doi.org/10.1016/j.coph.2019.07.006.
44. Sun W, Hesse S, Xu M, Childs RW, Zheng W, Williamson PR. 2018. "Real-Time" high-throughput drug and synergy testing for multidrug-resistant bacterial infection: a case report. Front Med (Lausanne) 5:267. https://doi.org/10.3389/fmed.2018.00267.
45. Lea WA, Xi J, Jadhav A, Lu L, Austin CP, Simeonov A, Eckenhoff RG. 2009. A high-throughput approach for identification of novel general anesthetics. PLoS One 4:e7150. https://doi.org/10.1371/journal.pone.0007150.
46. Titus SA, Li X, Southall N, Lu J, Inglese J, Brasch M, Austin CP, Zheng W.

2008. A cell-based PDE4 assay in 1536-well plate format for high-throughput screening. J Biomol Screen 13:609–618. https://doi.org/10.1177/1087057108319977.
47. Huang R, Southall N, Wang Y, Yasgar A, Shinn P, Jadhav A, Nguyen DT, Austin CP. 2011. The NCGC Pharmaceutical Collection: a comprehensive resource of clinically approved drugs enabling repurposing and chemical genomics. Sci Transl Med 3:80ps16. https://doi.org/10.1126/scitranslmed.3001862.
48. Clinical and Laboratory Standards Institute. 2017. Reference method for broth dilution antifungal susceptibility testing of yeasts; approved standard, 4th ed. CLSI document M27. Clinical and Laboratory Standards Institute, Wayne, PA.
49. Odds FC. 2003. Synergy, antagonism, and what the chequerboard puts between them. J Antimicrob Chemother 52:1. https://doi.org/10.1093/jac/dkg301.
50. Wang Y, Jadhav A, Southal N, Huang R, Nguyen DT. 2010. A grid algorithm for high throughput fitting of dose-response curve data. Curr Chem Genomics 4:57–66. https://doi.org/10.2174/1875397301004010057.
51. Hill AV. 1910. The possible effects of the aggregation of the molecules of haemoglobin on its dissociation curves. J Physiol 40:4–7.